9-2014

Within-row spacing sensing of maize plants using 3D computer vision

Akash D. Nakarmi
Iowa State University

Lie Tang
Iowa State University, lietang@iastate.edu

Within-row spacing sensing of maize plants using 3D computer vision

Abstract
Within-row plant spacing plays an important role in uniform distribution of water and nutrients among plants which affects the final crop yield. While manual in-field measurements of within-row plant spacing is time and labour intensive, little work has been done on an alternative automated process. We have attempted to develop an automatic system making use of a state-of-the-art 3D vision sensor that accurately measures within-row maize plant spacing. Misidentification of plants caused by low hanging canopies and doubles were reduced by processing multiple consecutive images at a time and selecting the best inter-plant distance calculated. Based on several small scale experiments in real fields, our system has been proven to measure the within-row maize plant spacing with a mean and standard deviation error of 1.60 cm and 2.19 cm, and a root mean squared error of 2.54 cm, respectively.

Keywords
Spacing sensing, Inter-plant spacing, Within-row, 3D computer vision, Time-of-flight

Comments
This is a manuscript of an article published as Nakarmi, Akash D., and Lie Tang. "Within-row spacing sensing of maize plants using 3D computer vision." *Biosystems Engineering* 125 (2014): 54-64. DOI: 10.1016/j.biosystemseng.2014.07.001. Posted with permission.

WITHIN-ROW SPACING SENSING OF CORN PLANTS USING 3D COMPUTER VISION

A. D. Nakarmi, L. Tang

The authors are **Akash D. Nakarmi,** Graduate Student, and **Lie Tang,** Associate Professor, Department of Agricultural and Biosystems Engineering, Iowa State University, Ames, IA, 50010, USA. **Corresponding author:** Lie Tang, Iowa State University, 203 Davidson Hall, Ames, IA, 50010; phone: 515-294-9778; e-mail: lietang@iastate.edu.

Abstract. *Within-row plant spacing plays an important role in uniform distribution of water and nutrients among plants which, affects the final crop yield. While manual in-field measurements of within-row plant spacing is time and labor intensive, little work has been done on an alternative automoted process. We have attempted to develop an automatic system making use of a state-of-the-art 3D vision sensor that accurately measures within-row corn plant spacing. The system is robust to outdoor illumination conditions and can be used at any time of day. The robustness to the illumination conditions was achieved by providing a provision for automatic selection of integration time during the image acquisition time. Misidentification of plants caused by long hanging canopies and doubles were reduced by processing multiple consecutive images at a time and selecting the best inter-plant distance calculated. Based on several small scale experiments in real fields, our system have been proven to measure the within-row corn plant spacing with a mean and standard deviation error of 1.60 cm and 2.19 cm, and a root mean squared error of 2.54 cm, respectively.*

Keywords. *Spacing Sensing, Inter-plant Spacing, Within-row, 3D Computer Vision, Time-of-flight*

INTRODUCTION

Plants compete among themselves for water and nutrients. Evenly spaced plants are necessary for uniform distribution of the water and nutrients required for proper growth. Researchers have studied the effect of plant standing variability (PSV) on final crop yield. Most notably, Nielsen (1991) reported that there was a reduction of about 62 kg/ha for every centimeter increase in standard deviation of within-row plant spacing. Doerge et al. (2001) found similar effects of plant space variability on grain yield, where they reported a loss of 84 kg/ha for every centimeter increase in standard deviation of within-row plant distribution. The effect of PSV on final crop yield however, is not conclusive as there exists some studies (Lauer et al., 2004 and Liu et al. 2004a) where the authors

reported that the effects of plant spacing variability on corn grain yield was negligible. Subsequent studies by Nielsen (2005) and Liu et al. (2004b), reported a yield loss of 54 kg/ha and 37 kg/ha, respectively, for every centimeter increase in standard deviation of plant spacing.

This work supplements traditional manual planter performance evaluation methods in favor of a new electronic one. Typically, manual measurements are carried about by laying down a tape measure along a crop row and recording inter-plant spacing on a notebook or an audio recorder. Manual methods are time and labor intensive as well as subject to human error. It takes approximately 25 minutes for a single worker to manually measure and record the inter-plant spacing of a typical crop row (61 m with 280-290 plants).

Tang et al. (2008a) and Tang et al. (2008b) used image processing techniques using top view images to automatically measure inter-plant spacing. Their approach relied solely on color information to detect plants on images, which resulted in error due to changes in outdoor illumination conditions. Also the accuracy of locating stem centers suffered, especially when the canopies of adjacent plants interconnected. Jian et al. (2009) developed a corn plant sensing system using a stereo camera with a 96 % correct detection rate. Nakarmi et. al (2012) took a different approach using a state-of-the-art 3D sensor based on time-of-flight (TOF) of light to automatically measure within-row corn plant spacing. The system did not rely on color information and used side view images to be able to accurately locate the stem centers on the images. A single image was processed at a time to detect stem centers which limited the system from detecting multiple plants growing together, and reduce the effect of long hanging canopies and outdoor illumination conditions. The system was tested on 9 m (30 ft.) long row segments and the reported misidentification rate was 2.2%.

In this paper, we are presenting a new approach to within-row corn plant spacing sensing system by processing three consecutive images at a time. The multi-view approach was instrumental in reducing the effect of direct sunlight reflecting off the plants and hanging canopies, as well as accurately detecting doubles. A provision for automatic selection of integration time was built into the system which was crucial for minimizing the effect of outdoor illumination conditions. The system performance was validated against manual measurements taken from multiple 61 m (200 ft.) long corn plant rows

MATERIALS AND METHODS

A three-wheeled cart, as depicted in figure 1, was designed such that the imaging area was covered to prevent direct sunlight from reflecting off the plants. A tunnel like structure was constructed and oriented so that during crop

measurements the row remained centered within it. The tunnel also ensured that the plant postures were not affected by wind blowing. The wall of the tunnel facing the camera was covered by a soft fabric material which resulted in uniform depth data on the wall. A high resolution, 4096 counts per revolution encoder was mounted on one of the rear wheels of the cart and was used to trigger image capturing. A leveler was placed in front of the wheel with the encoder to reduce the noise that might be caused by uneven soil surface.

(a) (b)

Figure 1. A three-wheeled data acquisition platform: (a) CAD model; and (b) Actual cart used.

A time-of-flight (TOF) of light based 3D camera, CamCube2^{TM} from PMD Technologies, Siegen, Germany, was mounted about 10 cm above the ground and at about 50 cm away from crop row. Each image was captured around 100 encoder counts which was approximately 5 cm along the crop row direction. With this from a typical 61 m (200 ft.) crop row, about 12 hundred images were collected. The corn plants were in v3-v4 (3-4 weeks) growth stage and herbicides were used kill weeds a week prior to capturing images from the field. The system was developed using C# programming language and Visual Studio 2010 development environment in Microsoft Windows 7 platform. The development of automatic algorithm for within-row corn plant spacing sensing was performed in the four-step process listed in table 1.

Table 1. Four step within-row corn plant spacing sensing algorithm

Image segmentation	a. Discard upper quarter of image to reduce the effect of long plant canopies b. Separate plants from background and soil using depth and amplitude values, respectively. c. Group foreground regions into separate plants and discard smaller regions
Stem center identification	a. Find Hough lines on segmented image b. Group Hough lines for each plant on the image c. Select Hough line that approximates stem center d. Trim plant regions around the Hough lines

Image mosaicking	a. Find common plant in three consecutive images b. If found, mosaic at common plant location, otherwise use encoder data to mosaic them
Inter-plant spacing measurement	a. Calculate variance of depth values along stem skeleton and use it as a score for each identified plant b. For two plants appearing in an image, sum the plant scores to assign score to the distance between them c. Calculate distance scores for the plants in every image they appear d. Use the distance with the lowest variance as the best available distance between the plants

First, the captured images were segmented to separate plants from the background using the distance data. In the next step, the plant stem centers were localized. The images were then mosaicked together and finally inter-plant spacing was computed. For the sake of completeness, the operating principle of the 3D camera will be presented in the next section and a detailed description of the algorithm will be presented in the following sections.

OPERATING PRINCIPLE AND CHARACTERISTICS OF CAMCUBE2™

CamCube2™ sends out modulated light waves from light emitting diodes (LEDs) and the imaging sensor measures the phase shift of returned signal at each pixel. The returned signal amplitude A is smaller than the emitted signal amplitude E as shown in figure 2. The received signal is modulated four times per cycle with each sample shifted by 90° phase angle. The phase shift φ and the distance are then calculated using equations 1 and 2 respectively.

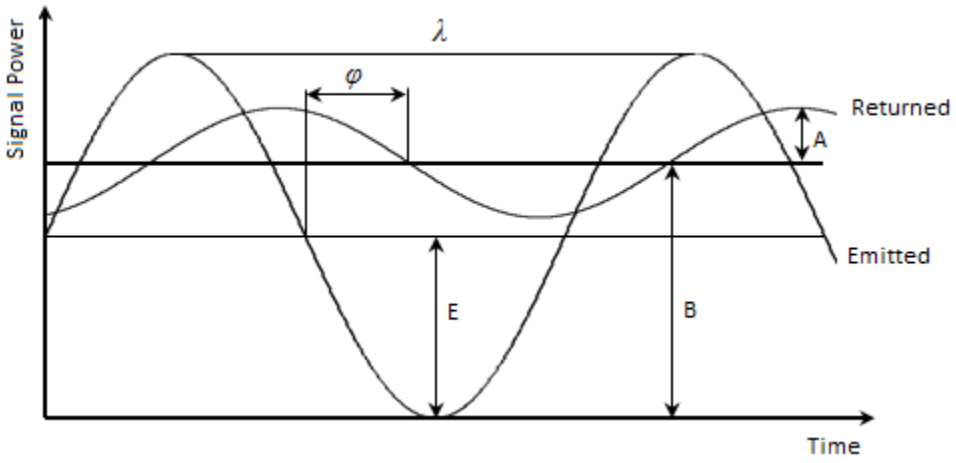

Figure 2. Operating principle of time-of-flight (TOF) of light based 3D sensor

$$\varphi = \arctan\left(\frac{A_0 - A_2}{A_1 - A_3}\right) \quad (1)$$

$$R = \frac{c}{4\pi f_{\text{mod}}}\varphi = \frac{\varphi}{2\pi}\frac{\lambda}{2} \quad (2)$$

where A_0, A_1, A_2 and A_3 are four samples of received signal, c is the speed of light, f_{mod} is modulating frequency and λ is its wavelength (Ringbeck, 2007). CamCube2^{TM} camera comes pre-calibrated and by default operates at 20 MHz modulating frequency. Suppression of background illumination (SBI) implemented in the camera model allows the sensor to automatically correct for environmental fluctuations such as illumination conditions and makes it suitable for outdoor applications.

CamCube2^{TM} and other similar TOF based sensors are superior to conventional stereo vision systems as they do not rely on non-uniform texture feature for non-ambiguous disparity map generation. This feature is particularly useful for the application as plant canopies often present somewhat uniform texture. The sensor captures spatial data in Cartesian coordinates with its origin at the center of the frontal face of the camera. The camera also captures amplitude image which contains for each pixel a value representing the strength of the reflected signal by the object. The amplitude values are low when the strengths of the reflected signals are weak. The camera has a rather small field of view (FOV), 40° (h) × 40° (v) and captures images with 204 × 204 pixels resolution.

Integration time is one of the most important and only available internal camera parameter that could be adjusted. It describes the time period in which incoming photons are detected for one measurement cycle, in order to derive phase shift and the corresponding distance. If the integration time is set too low, the amplitudes of related pixels decrease and distances for distance objects cannot be measured. On the other hand, if the integration time is too high, oversaturation is observed and measurements fail. Therefore, integration times needs to be carefully selected before acquiring images. A mechanism was built into the system which sampled images at varying integration times of the same scene with two or more plants. Five images were taken per integration time, and the average distance between any two plants was calculated and compared to the hand-measured distance. The integration time that gave the smallest error between the hand-measured distance and the calculated average distance was chosen as the best suitable integration time to be used at the time of collecting field data. This was done for each row, which was a crucial step for elimination of the effect of outdoor illumination conditions.

IMAGE SEGMENTATION

The captured images were radially distorted which was corrected using Equations 3 and 4.

$$x_i = \frac{f}{p} \times \frac{x_w}{\left(z_w + c\right)} \tag{3}$$

$$y_i = \frac{f}{p} \times \frac{y_w}{\left(z_w + c\right)} \tag{4}$$

where, (x_i, y_i) are the corrected image coordinates corresponding to the scene points (x_w, y_w), f is the focal length and p is the pixel-pitch of the camera, and c is the distance from the frontal face of the camera to the imaging area inside the camera. The corrected images were then processed to separate plants from the background and soil. The top quarter of the images were discarded to reduce the effect of leaves in plant localization and stem center identification. A depth threshold at 5 cm in front of the tunnel wall was used to segment the middle half of the image. The fact that the lower quarter of the image mostly contained soil region and that amplitude values of soil pixels were significantly lower than those of plant pixels was used to implement an amplitude threshold to separate plant regions from the soil. Basically, depth and amplitude values were used to segment plants from the background and the soil, respectively. Region growing algorithms were used to group connected pixels together and smaller isolated regions were removed (Heijden, 1995). Samples of the depth, amplitude, and background, soil removed and final segmented images are shown in figure 3.

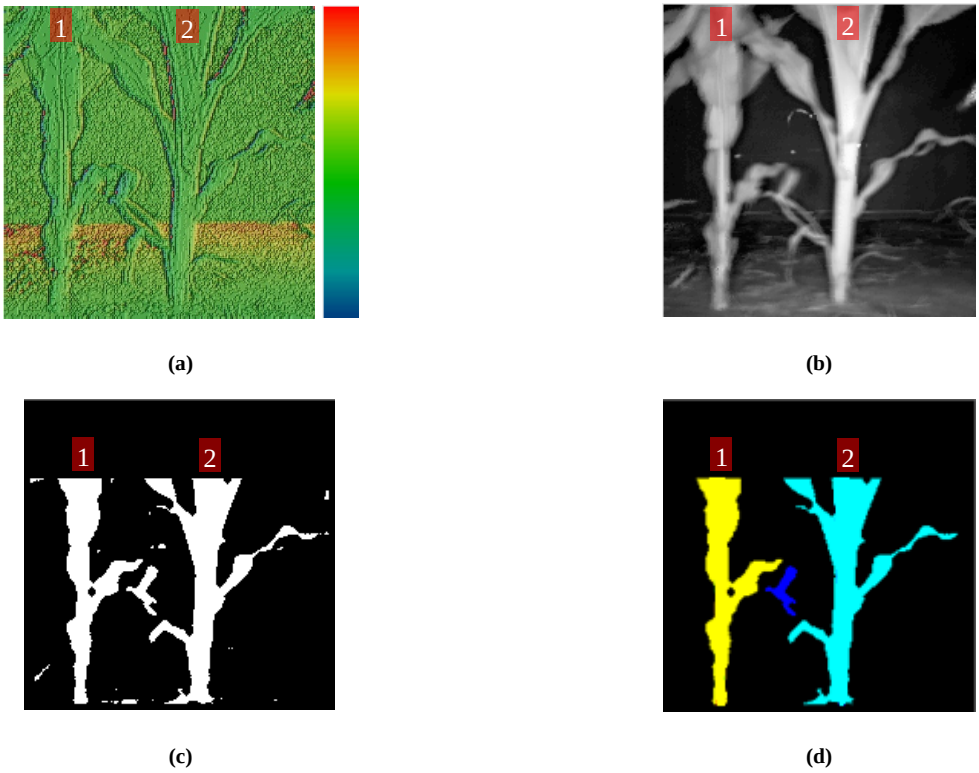

Figure 3. Image segmentation: (a) depth image; (b) amplitude image; (c) image with upper quarter discarded, background and soil removed; (d) final segmented image

STEM CENTER IDENTIFICATION

For stem center identification Hough lines were found on segmented image. Search for the Hough lines were limited to $\pm 15^{\circ}$ from the vertical, which allowed for the identification of plants inclined up to 15° left and right of the vertical and also improved the computation time. Identified Hough lines were grouped together based on their proximity. X values of the lower ends of the Hough lines in each group were sorted and one with the median value was used as the best line passing through the center of the plant stem. The plant regions were then trimmed around the best Hough line. Skeleton of the trimmed plant regions were computed and the lower most point on the skeleton was used as the stem center. Samples of segmented image, identified Hough lines, plant regions trimmed around the best Hough lines and skeletons of the trimmed plant regions are illustrated in figure 4.

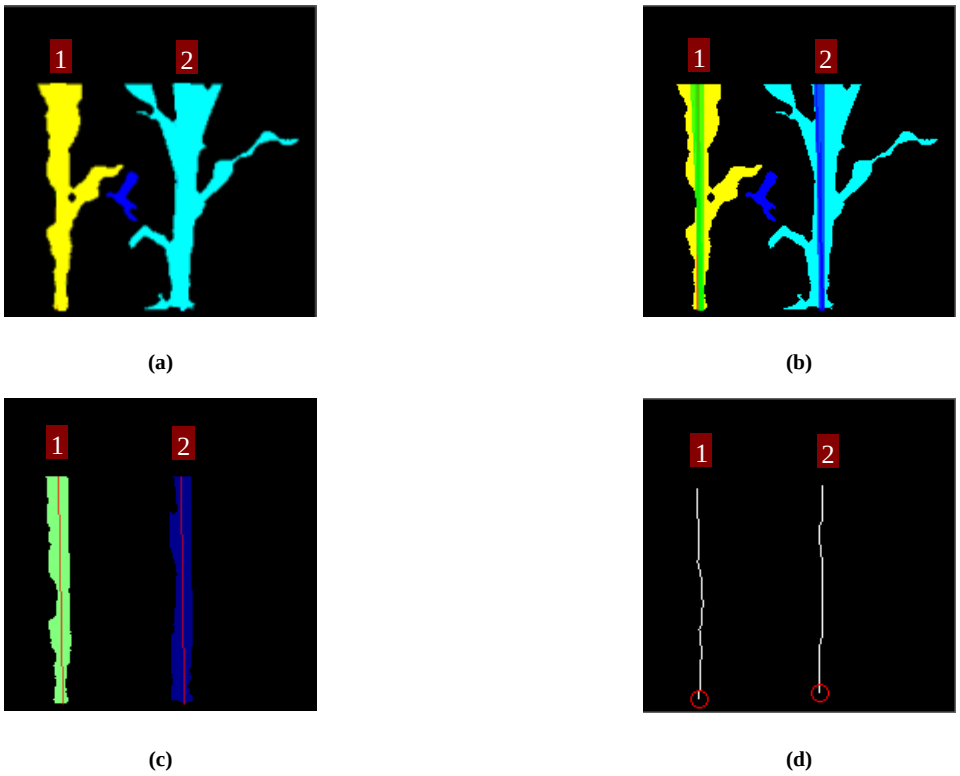

Figure 4. Stem center identification: (a) segmented image; (b) identified Hough lines; (c) plant regions trimmed around the best Hough lines; (d) skeletons of trimmed plant regions

CHALLENGES IN ACCURATELY LOCATING STEM CENTERS

Figure 5 depicts two typical cases which were required to be resolved for the robustness in stem center identification and hence for improving inter-plant spacing measurement accuracy of the system. In the first case, it was observed that plant leaves at times occluded the stems, which prevented the system from accurately locating the stem center. When the adjacent images were processed, the system however, was able to locate the stem centers without difficulty. The scenario is illustrated in figure 5a, where the system had difficulty in accurately locating plant 2 in the middle image. But it was able to detect the plant in the left and the right images. In the second case, a few cases of multiple plants growing together were observed. The system detected the plants as one plant on the first two images shown in figure 5b, while it was able to detect them as two plants in the third image. In order to resolve the issues for subsequent image mosaicking and inter-plant spacing measurement steps, an algorithm was developed to multiple images, an image in hand and its two neighbors.

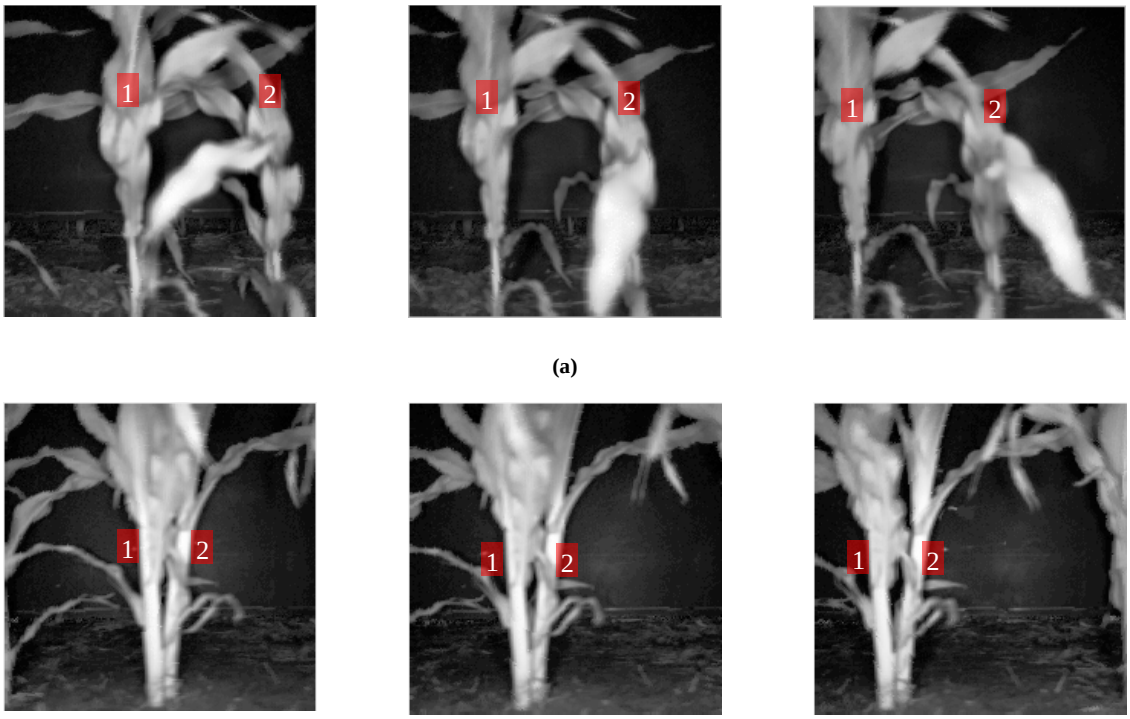

Figure 5. Typical issues in stem center identification: (a) plant leaves occluding a stem; (b) multiple plants growing together

IMAGE MOSAICKING

The images were stitched together to form a mosaicked image. When the images were mosaicked based on encoder data alone the mosaicked image appeared unrealistic (Fig. 6). The mosaicking locations were chosen at the middle of the images. The vertical lines at the top of the image represent the mosaicking locations. Plants 2, 3, 4, and 8 appeared to be cut-off during mosaicking process.

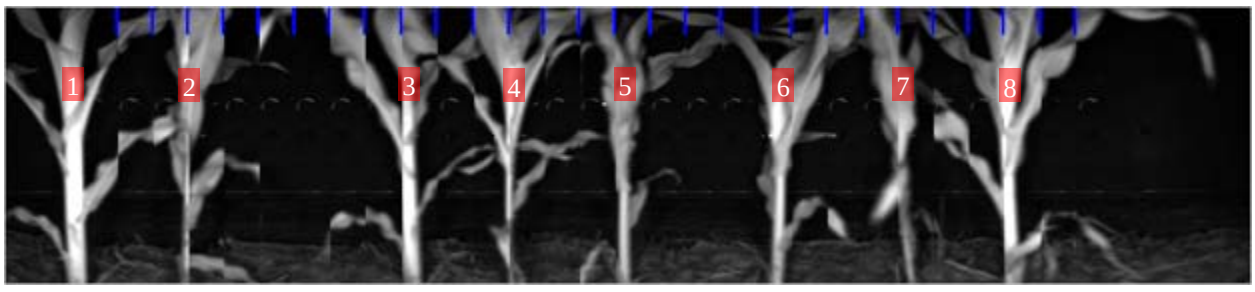

Figure 6. Image mosaicking based on encoder data alone

Therefore, a different approach was taken to mosaic images where in each step three images were considered for mosaicking. Image grouping scheme is shown in figure 7. The identified stem locations were used to mosaic the images where possible, and encoder data was used when stem location information was not available. The multi-view approach was used to account for cases shown in figure 5 as well as to improve distance calculation accuracy, which will be discussed in the next section. A sample mosaicked image is shown in figure 8. The mosaicking scheme was based on the flowchart shown in figure 9.

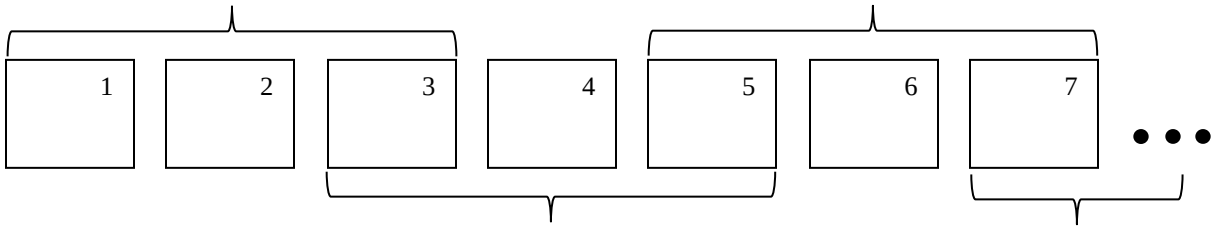

Figure 7. Image grouping: three images at a time

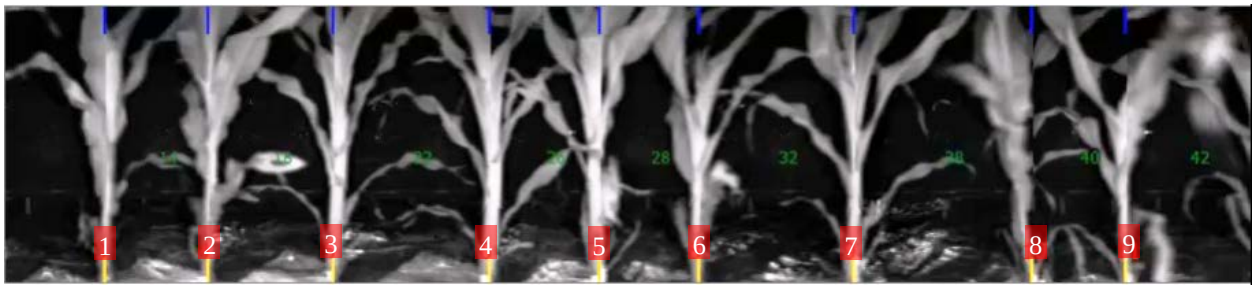

Figure 8. A sample mosaicked image based on the new mosaicking scheme

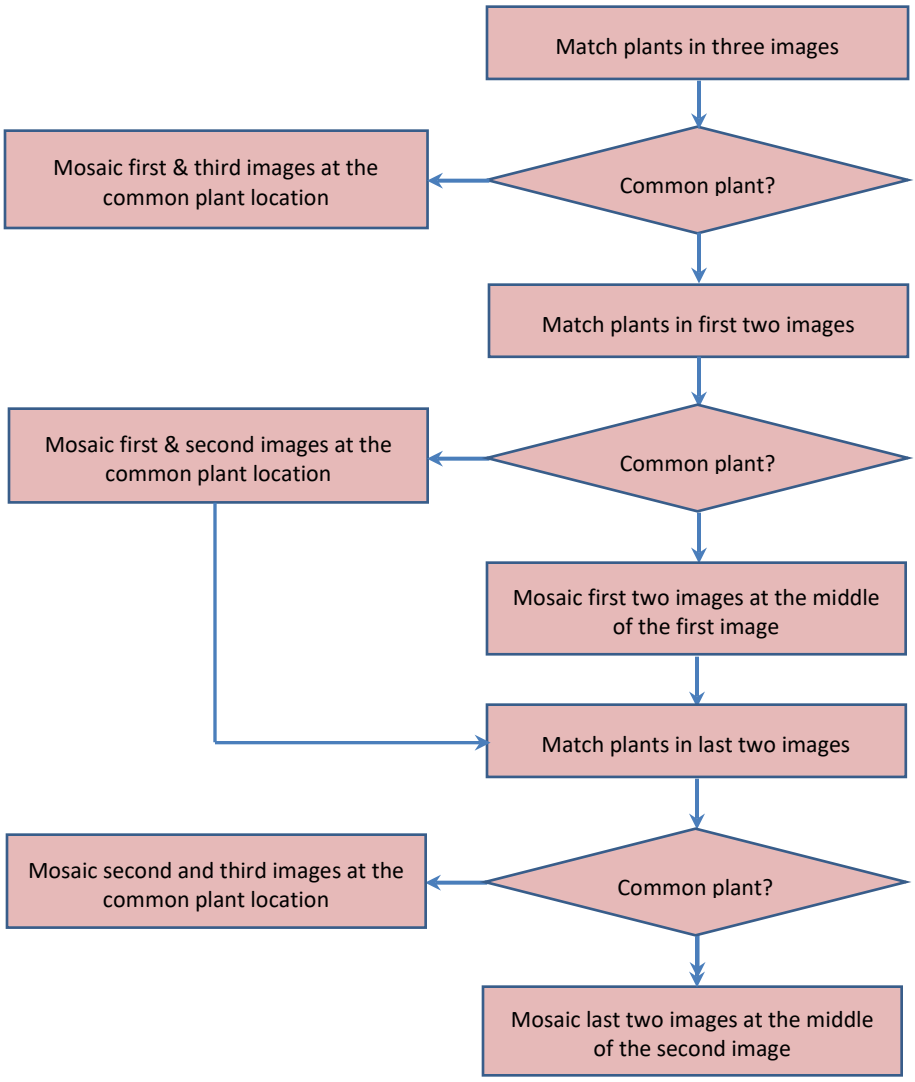

Figure 9. Image mosaicking scheme

First, a common plant was searched in the three images in hand. The encoder data was used to define search regions on the second and third images for the plant identified in the first image. If it was identified, the first and the third images were stitched at the common plant location and the mosaicked image was formed from these two images, while the second image was completely discarded for the image mosaicking purpose. Figure 10 illustrates the scenario where (a) a common plant in the three images is marked and (b) identified stem locations are marked by lower lines and a mosaic location is marked by the upper line.

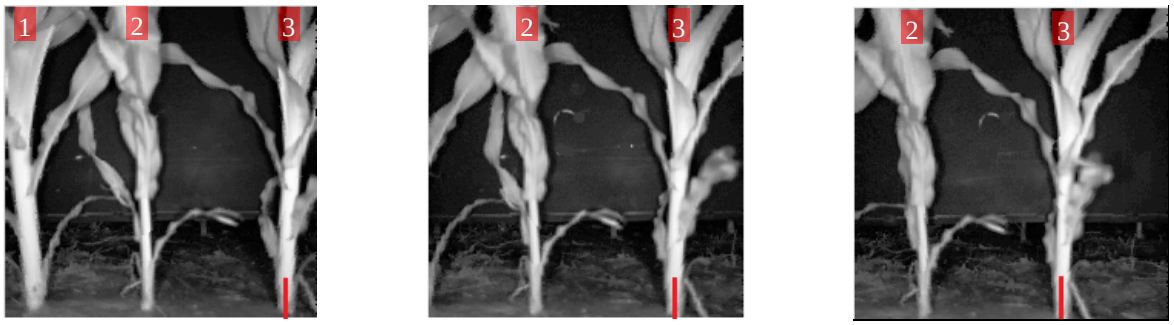

(a)

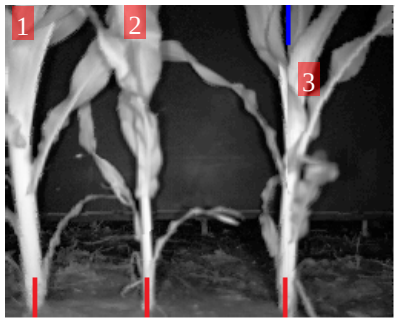

(b)

Figure 10. Image mosaicking when there is a common plant: (a) three consecutive images with a common plant; (b) mosaicked image formed by stitching the first and the third images

When a common plant was not identified in all three images, a common plant was searched between the first and the second images. If it was identified, the two images were stitched at the common plant location. In order to stitch the second and the third image, a mosaic location on the third image was determined as a location corresponding to the middle of the second image. For this purpose, encoder data was used to calculate the translation between the two images along the crop row direction. The case is depicted in figure 11. Similar scheme was used, when there was no common plant between the first and the second images.

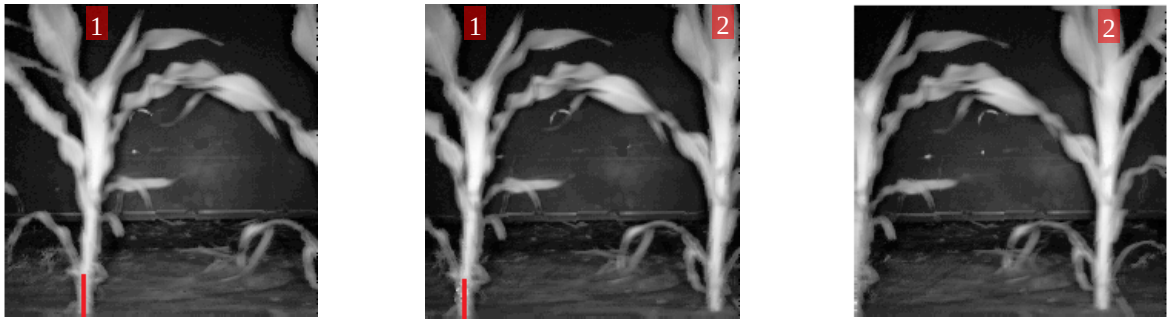

(a)

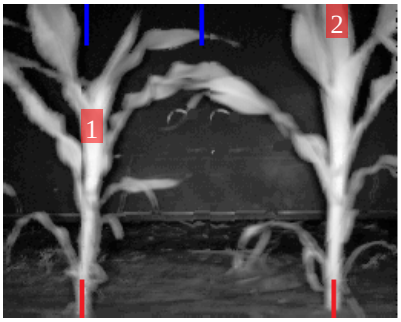

(b)

Figure 11. Image mosaicking when there is a common plant between two images: (a) three consecutive images with a common plant in the first and the second images; (b) mosaicked image formed by stitching the first and the second images at their common plant location (upper left line) and, the second and the third images at the middle of the second image and its corresponding location in the third image (upper right line)

When there was not a common plant between all three images, the images were mosaicked entirely based on the encoder data In the example shown in figure 12, the first and the second images were mosaicked at the middle of the first image and its corresponding location, estimated using encoder data, on the second image. Similarly, the second and the third images were mosaicked at the middle of the second image and its corresponding location on the third image.

(a)

(b)

Figure 12. Image mosaicking when there is no common plant between images: (a) three consecutive images with no common plant between them (b) mosaicked image formed by stitching the first and the second images at the middle of the first image and its corresponding location in the second image (upper left line) and, the second and the third images at the middle of the second image and its corresponding location in the third image (upper right line)

INTER-PLANT SPACING MEASUREMENT

The multi-view approach was used in used to calculate the distances between the plants as well. The idea was to calculate distances between any two plants in all the images in which they were visible and pick the one that the algorithm indicated as the best. The identified stems were assigned with scores based on the variation of depth values along the skeletons up to 5 cm up from the lowermost point of the skeleton. In absence of noise, due to occluding leaves, direct sunlight etc., depth variance along a stem was expected to be small. Smaller the depth variance higher is the chance of having good inter-plant spacing measurement. While measuring the distances between any two plants, the depth variances of the plants were summed up to assign scores to the distance measured between them. Every time the same two plants appeared on different images, the distance scores were saved, and the distance with the lowest score was selected to be the best available measurement. The process is illustrated in figure 13. The distance measured between the plants on the first image was selected as the best available distance as the calculated depth variance along the stems was the lowest. The depth variance on the third image was the highest due to the leaf that occluded the stem of the first plant. The distance between the plants measured in the field was 20.21 cm, and the system measured distance was 20.09 cm.

(a) (b) (c)

Figure 13. Inter-plant spacing measurement using multi-view approach: (a) with depth variance of 6.32 and measured distance 20.09 cm; (b) with depth variance of 10.87 and measured distance 20.38 cm; (c) with depth variance of 4070.37 and measured distance 26.41 cm. In-field manual measurement was 20.21 cm which is closest to the distance selected by the system in the first image

The system measurements were compared against in-field manual measurements to calculate mean and standard deviation of error. Misidentification rate was calculated to determine the percentage of manual correction. The misidentification rate was computed using Equation 5.

$$R_m = \frac{N_m + N_f}{N} \tag{5}$$

where N_m is total number of missed plants, N_f is total number of false detection and N is total number of plants in a row.

RESULTS AND DISCUSSION

Four 200 ft. long corn rows were used for the performance evaluation of the system. Data collection was done in June, 2011 on a test field in Illinois.

It was found that the false detection was none for all the rows, while the system missed to detect the plants which were shorter than the threshold used. The average mean±standard deviation of error was 1.60±2.19 cm and root mean squared error (RMSE) was 2.54 cm. The results of the experiment are listed in table 2.

Table 2. Average within-row corn plant distance measurement error.

Row	No. of plants (N)	No. of detections	No. of missed plants (N_m)	No. of false detections (N_f)	Misidentification rate (R_m)	Mean±Std.Deviation of error (cm)	RMSE (cm)

1	288	284	4	0	1.38 %	1.20±1.87	2.12
2	273	265	8	0	2.93 %	1.14±1.67	2.23
3	270	267	3	0	1.10 %	2.65±2.88	3.25
4	266	264	2	0	0.75 %	1.43±2.36	2.77
Average	274				1.54 %	1.60±2.19	2.54

The average detection rate (1.54 %) of the system stands well above the detected rate reported by Jian et al. (2009). The system reported by Tang et al. (2008a) and Tang et al. (2008b) relied solely on color information to detect plants on images, which resulted in errors due to changes in outdoor illumination conditions. On the other hand, the system presented in this paper is robust towards illumination variations. While the resolution of the images (204 x 204 pixels) captured by the ToF camera is far less compared to the resolution that can be achieved with stereo heads, the accuracy of the 3D information that can be achieved with the ToF sensor stands well above that of the stereo head. This gives ToF sensors a direct advantage over stereo cameras in applications such as inter-plant spacing sensing.

The tunnel like structure was designed not only to prevent direct sunlight from shining on the plants, but also to reduce the effects of wind. While in the current form, the cart is pushed which is still a labor intensive process, it is more a prototype to prove the concept. The most important achievement lies in the time efficiency of the system. The time of 6.5 minutes spent on capturing and processing images from a typical 61 m (200 ft.) crop row is only about 1/4th of the time cost in manual measurement. Furthermore, this imaging platform can also be straightforwardly modified so that it can be pulled by a tractor or a similar agricultural vehicle.

CONCLUSIONS

With the multi-view approach, the system was able to resolve issues imposed by long hanging plant canopies and doubles (two plants growing together). The multi-view approach also helped to improve the accuracy of the stem center identification, and hence inter-plant spacing measurements. The average misidentification rate was 1.54 % with no false detections. The missed plants were mostly the short ones. The presence of shorter weeds and dead but standing weeds did not affect the performance of the system. The system took about 3 minutes to capture images from a typical 61 m (200 ft.) crop row containing an average of 275 plants and about 3 and ½ minutes to process them which was significantly faster compared to 25 minutes required to collect manual measurements.

The use of TOF camera as opposed to conventional stereo camera proved advantageous as TOF camera did not rely on non-uniform texture feature for non-ambiguous disparity map generation which make the system robust to

outdoor illumination conditions. However, the imaging area was needed to be properly covered so that direct sunlight did not shed on plants. It was noticed that integration time of the camera required to be adjusted depending on the sunlight conditions so as to capture better data. While in the morning and the evening hours an integration time of 800 - 1000 μs was found to give better data, during the middle of the day when the sunlight intensity was very strong an integration time of 300 - 500 μs was used. Robustness to outdoor illumination conditions was further achieved through the multi-view approach taken for the stem location identification, which allowed the system to select the most accurately measured inter-plant distance.

REFERENCES

Doerge, T., Hall, T. and Gardner, D. 2001. New Research Confirms Benefits of Improved Plant Spacing in Corn. Pioneer Hi-Bred. Available at: https://www.pioneer.com/home/site/us/agronomy/library. Accessed 08 May 2012.

Heijden, F. van der. 1995. *Image Based Measurement Systems: Object Recognition and Parameter Estimation.* West Sussex, England: John Wiley and Sons.

Jian, J. and Tang, L. 2009. Corn Plant Sensing Using Real-time Stereo Vision. *Journal of Field Robotics. 26(6-7): 591-608.*

Lauer, J. and Rankin, M. 2004. Corn Response to Within-row Plant Spacing Variation. *Agron. J., 96: 1464-1468*.

Liu, W., Tollenaar, M., Stewart, G. and Deen, W. 2004a. Within-row Plant Spacing Variability Does Not Affect Corn Yield. *Agron. J., 96: 275-280*.

Liu, W., Tollenaar, M., Stewart, G. and Deen, W. 2004b. Impact of Planter Type, Planting Seed and Tillage on Stand Uniformity and Yield of Corn. *Agron. J., 96: 1668-1672*.

Nakarmi, A.D. and Tang, L. 2012. Automatic Inter-plant Spacing Sensing at Early Growth Stages using a 3D Vision Sensor. *Computers and Electronics in Agriculture, 82: 23-31*.

Nielsen, R.L. 1991 (Rev. 2001). Stand Establishment Variability in Corn. Purdue University, Agronomy Department. Publication AGRY-91-01. Available online at http://www.agry.purdue.edu/ext/pubs/AGRY-91-01_v5.pdf. (URL verified 05/07/2012).

Nielsen, R.L. 2004 (rev. 2005). Effect of Plant Spacing Variability on Corn Grain Yield. Purdue University, Agronomy Department. Available online at http://www.agry.purdue.edu/ext/corn/research/psv/Report2005.pdf (URL verified 05/08/2012).

RingBeck, T. and Hagebeuker, B. 2007. A 3D Time of Flight Camera for Object Detection. *Measurement,* 9(2), 636-642. Available online at http://ifm.hu/obj/O1D_Paper-PMD.pdf (URL verified 05/08/2012)

Tang, L. and Tian, L. F. 2008a. Plant Identification in Mosaicked Crop Row Images for Automatic Emerged Corn Plant Spacing Sensing. *Transactions of ASABE. 51 (6): 2181-2191.*

Tang, L. and Tian, L. F. 2008b. Real-time Crop Row Image Reconstruction for Automatic Emerged Plant Spacing Measurement. *Transactions of ASABE. 51(3): 1079-1087.*